ELSEVIER

Journal of Hydrology 215 (1999) 202–214

Journal of Hydrology

Modeling gravity driven unstable flow in a water repellent soil

H.V. Nguyen[a,*], J.L. Nieber[a], C.J. Ritsema[b], L.W. Dekker[b], T.S. Steenhuis[c]

[a]*Department of Biosystems and Agricultural Engineering, University of Minnesota, St. Paul, USA.*
[b]*DLO Winand Staring Centre for Integrated Land, Soil and Water Research, Wageningen, The Netherlands*
[c]*Department of Agricultural and Biological Engineering, Cornell University, Ithaca, NY, USA.*

Received 21 February 1998; accepted 24 August 1998

Abstract

One mechanism for the initiation of unstable flow in porous media is a condition of hydrophobicity of the solid phase. Recent continuous and nondestructive measurements of water content distribution in a 200 cm wide by 70 cm deep trench of a Netherlands' field soil containing a hydrophobic layer, reveals a complicated wetting pattern with fingered flow being quite prevalent. The soil profile consists of a humic top layer, a second layer consisting of hydrophobic sand, and a hydrophilic sandy layer at the bottom of the soil profile. In this paper we show our attempts to simulate the unstable flow pattern observed in the field using a numerical solution developed for modeling gravity-driven unstable flow. The unstable flow simulation method employs a globally mass conservative finite element solution of the Richards equation applied to the soil trench. The overall patterns of simulated saturation are similar to those of observed saturation. Statistical analysis shows that pointwise predicted saturation is reasonably close to the observed.

Keywords: Unstable flow; Hydrophobic soil; Finite element method; Modeling

1. Introduction

Sharp and stable wetting fronts, predicted by the Green and Ampt (1911) and Philip (1969) theories of infiltration, have been observed in laboratory studies of water infiltrating into dry homogeneous porous media. Generally these observations have been made when the porous media are in narrow columns. In contrast, in many field and laboratory columns/chambers of larger width, the observed water movement seems to contradict these classical theories. Instead of advancing as a smooth front, water penetrates into the soil at certain locations and grows through narrow wetting columns while the intervening soil remains dry during infiltration and redistribution periods. This observed phenomenon, defined as unstable flow or fingered flow, is considered to be one form of preferential flow (Beven, 1991). When unstable flow occurs, water and solutes move in pathways through the vadose zone at velocities that are close to the saturated hydraulic conductivity divided by the water content at saturation (Glass et al., 1988). This by-passing flow can significantly increase the amount of harmful substances moving to underlying ground water (Glass et al., 1988), and also can cause a reduction of nutrients and water available for plant growth (Jamison, 1945).

Philip(1975) states the criterion for development of unstable flow to be that the vertical water pressure gradient oppose the gravitational field gradient. According to Philip, this condition for unstable flow

* Corresponding author. Tel.: 001 612 625 6724; Fax: 001 612 624 3005; e-mail: hnguyen@s1./arc.umn.edu

0022-1694/99/$ - see front matter
PII: S0022-1694(98)00269-8

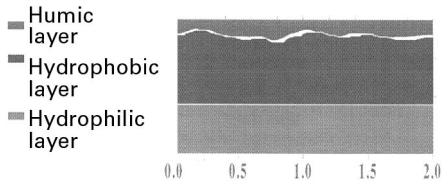

Fig. 1. The soil profile at the Ouddrop site, the Netherlands.

can occur under any of the following conditions: hydrophobic or very dry soil conditions; an increase in hydraulic conductivity with depth; and compression of air ahead of the wetting front. While any of these conditions are requisite for unstable flow to occur, they are not sufficient. The additional necessary condition to achieve sufficiency is that the water retention function must be hysteretic (Glass et al., 1989b; Nieber, 1996).

Evidence of unstable flow in field soils were reported by numerous researchers, including Starr et al. (1978), van Ommen et al. (1988), Ghodrati and Jury (1990), van Dam et al. (1990), Pendexter and Furbish (1991), Hendrickx and Dekker (1991), Hendrickx et al. (1993), Dekker and Ritsema (1994), and Ritsema et al. (1996, 1997, 1998). Many of these researchers observed unstable flow in soil profiles having a hydrophobic layer, and recognized this as meeting one of the conditions for flow instability (Philip, 1975).

Nieber (1996) performed a numerical solution for unstable flow in homogeneous soils. The method applied the conventional Galerkin finite element method to the mixed form of the Richards equation. The system of algebraic equations is derived by fully implicit time discretization, and the modified Picard procedure is used to solve the nonlinear systems. An upstream weighting procedure as described by Dalen (1976) is used to determine the internodal hydraulic conductivities. With this numerical solution Nieber (1996) simulated flow in a single finger, and found that the simulated finger widths were close to those obtained from the theory described by Glass et al. (1989a). He pointed out that an initial perturbation in the wetting front will grow if the water entry capillary pressure on the main wetting curve is less than the air entry capillary pressure on the main drainage curve. This condition will usually exist for hydrophobic soils.

The study reported in the present paper uses the numerical solution method described by Nieber (1996) applied to the simulation of unstable flow in a field soil containing a hydrophobic layer. Tests of

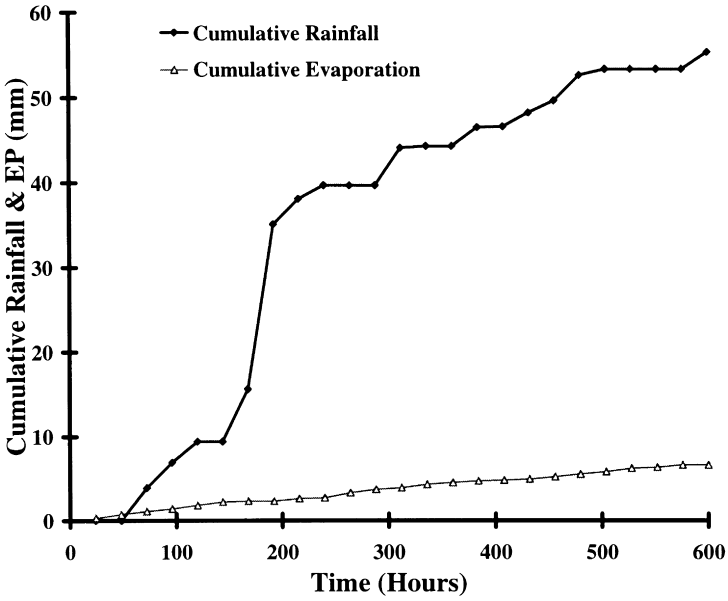

Fig. 2. Cumulative rainfall and evaporation amounts.

Table 1
Soil properties and van Genuchten parameters determined by RETC model.

Parameters	Humic Layer		Hydrophobic Layer		Hydrophilic Layer	
Curve	Wetting	Drainage	Wetting	Drainage	Wetting	Drainage
θ_r (%)	0.08	0.08	0.04	0.04	0.02	0.02
θ_s (%)	0.435	0.435	0.365	0.365	0.40	0.40
K_S (m day^{-1})	1.00	1.00	1.00	1.00	2.20	2.20
n	1.99	1.80	35.45	4.49	1.92	3.02
α (m^{-1})	2.47	1.63	20.90	1.90	11.65	2.93

how well the numerical simulations mimic the observed field data are based on qualitative comparisons of observed and simulated moisture patterns, and on quantitative statistical analyses of differences in moisture contents at measurement points.

2. Materials and methods

The experimental site is located near the village of Ouddorp in the coastal dune area in the southwestern part of the Netherlands. The soil has a sandy texture and consists of three layers: a humic layer with an average thickness of 10 cm, a hydrophobic layer of 30 cm average thickness, and underlying the hydrophobic layer the sand is hydrophilic and this extends to the water table (Fig. 1; note that only the top 30 cm of the hydrophilic layer is shown). The wavy interface between the top and second layers is apparent in the interpolations of the saturation as measured by the TDR probes in the soil profile on a dry day (1:00 am December 1, 1994). The interface between the hydrophobic and hydrophilic layers is assumed horizontal.

The soil water measurements in the trench extend over a surface that is 200 cm wide by 70 cm deep from the soil surface. The moisture content was monitored using a stand-alone TDR measurement device to which 98 sensors were connected. Fourteen probes were placed 15 cm apart horizontally at depths of 4, 12, 20, 30, 40, 55, and 70 cm. Soil moisture content was automatically recorded every three hrs at the 98 sensors for a period of 25 days. Rainfall, when it occurred, was measured at 15 min intervals. In addition, potential evaporation was recorded daily and water table depth was recorded hourly. Fig. 2 shows the cumulative rainfall and potential evaporation amounts versus time for a 25 day period in the record. The water table level was always well below the lowest row of TDR sensors during this observation period.

2.1. Soil hydraulic properties

Predicting soil hydraulic properties involved determining the main wetting and drainage water retention and hydraulic conductivity curves. The main wetting and drainage curves were determined by the hanging water column method (Stolte et al., 1992) from separate samples of the three soil layers. The unsaturated hydraulic conductivity curves were determined with the method of modified evaporation of Wind as described by Tamari et al. (1993), and the saturated hydraulic conductivity was determined with the constant-head method (Klute, 1986).

The computer program RETC (RETention Curve, van Genuchten et al., 1991) was used to optimize the van Genuchten soil parameters (n and α in Table 1) based on the relationships between measured water content, capillary pressure and hydraulic conductivity. Figs. 3(a)–(c), compare the experimental main drainage and boundary wetting scanning water retention curves with the curves predicted by the RETC model for the humic, hydrophobic, and hydrophilic layers, respectively.

It is seen in Fig. 3(a), that for the humic layer the RETC model under-predicted water content for the high values of capillary pressure. For the flow simulations to be discussed later it will be shown that the measured water content in the humic layer was found to remain relatively high during the simulation period. Therefore, the lack of fit of the water content function

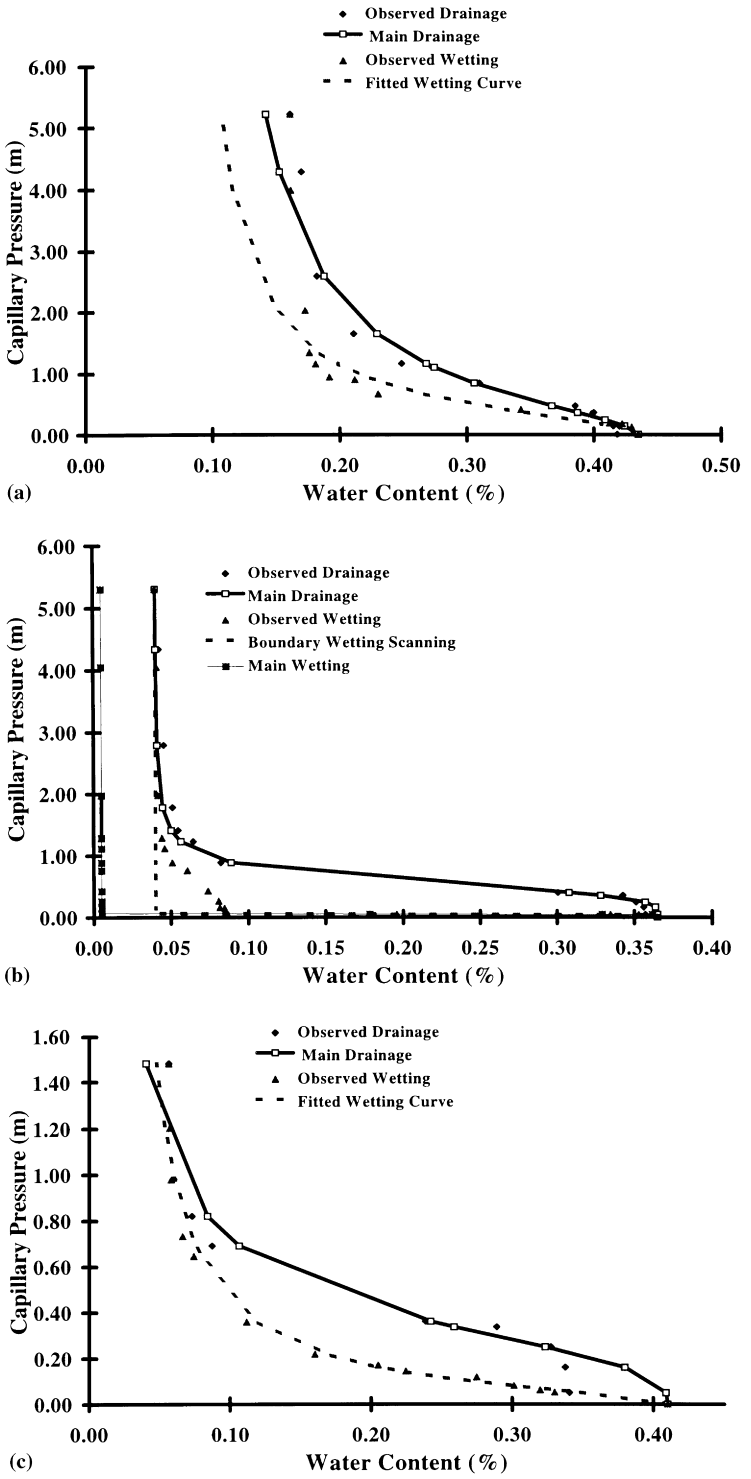

Fig. 3. The main drainage and wetting water retention curves for (a) the humic layer (b) the hydrophobic layer (c) the hydrophilic layer.

at the low end of the water content range should not lead to large inaccuracies of simulated flows in the humic layer.

For the hydrophobic layer the main drainage and boundary wetting scanning curves are both relatively steep (Fig. 3(b)). The relative steepness of the boundary wetting scanning curve is similar to that found for hydrophilic soils with narrow coarse-textured particle size distributions (Liu et al., 1994). At Ouddorp, the sand is not coarse-textured, nor is the particle size distribution narrow. Instead the steep curve occurs because of the hydrophobicity of the soil. The main wetting curve shown in Fig. 3(b) was not measured, but was estimated from the characteristics of the boundary wetting scanning curve.

In contrast to the water retention characteristic for the hydrophobic layer, the water retention curves for the hydrophilic layer (Fig. 3(c)) have much smaller slopes. This appears to be the case although the texture of the hydrophilic layer is similar to that of the hydrophobic layer. The van Genuchten model appears to provide a good fit to the main drainage and the boundary wetting scanning curves for the hydrophilic soil.

Fig. 4(a)–(c) show the hydraulic conductivity curves for the three layers. The van Genuchten model for unsaturated hydraulic conductivity underpredicted the unsaturated hydraulic conductivity for both the humic and hydrophobic layers, and overpredicted the unsaturated hydraulic conductivity for the hydrophilic layer. No attempt was made to improve the fit of these unsaturated hydraulic conductivity functions. At present we are uncertain as to the significance of the lack of fit of the unsaturated hydraulic conductivity function on flow simulation results.

Table 1 summarizes the soil moisture and hydraulic properties, and the van Genuchten parameters determined by the RETC model. In Table 1, θ_r and θ_s are the residual and saturated volumetric water content, respectively, K_s is the saturated hydraulic conductivity and n and α are porous media dependent parameters.

2.2. Numerical solution

The single-phase flow of water for the two-dimensional case can be represented by the Richards equation:

$$\frac{\partial\theta}{\partial t} - \frac{\partial}{\partial x}\left(K\frac{\partial h}{\partial x}\right) - \frac{\partial}{\partial z}\left(K\frac{\partial h}{\partial z}\right) - \frac{\partial K}{\partial z} = 0 \qquad (1)$$

where θ is the volumetric water content [m^3/m^3], h is the water pressure head [m], $K(\theta)$ is the unsaturated hydraulic conductivity [m/min], x and z are Cartesian coordinates with z being the vertical coordinate pointed upward [m], and t is time [min].

In addition to this primary equation, we require auxiliary relationships for the variables and the parameters in Eq. 1. For the main drainage function, the boundary wetting scanning function, and the main wetting function, these equations are,

$$h_c = -h \qquad 2(a)$$

$$\theta = (\theta_s - \theta_j)\left(\frac{1}{1+(\alpha_j h_c)^{n_j}}\right)^{1-\frac{1}{nj}} + \theta_j, j = d, w, adw \qquad 2(b)$$

$$S_e = \frac{\theta - \theta_r}{\theta_s - \theta_r} \qquad 2(c)$$

$$K = K(K_s, S_e) = K_s S_e^{\frac{1}{2}}\left[1 - \left(1 - S_e^{\frac{n_j}{n_j-1}}\right)^{1-\frac{1}{n_j}}\right]^2, S_e > 0, j = d, w, adw \qquad 2(d)$$

$$K = 0, S_e \le 0 \qquad 2(e)$$

where h_c is the capillary pressure head [m], K_s is the saturated hydraulic conductivity [m/min], S_e is the effective saturation [1], θ_s is the saturated water content [m^3/m^3], θ_r is the residual water content on both the main drainage function and the boundary wetting scanning function [m^3/m^3], θ_{adw} is the air-dry water content on the main wetting function [m^3/m^3], and α_j [m^{-1}] and n_j [1] are porous media dependent parameters for the main drainage function ($j = d$), boundary wetting scanning function ($j = w$), and main wetting function ($j = adw$). The relation given by Eq. 2(a) is obtained because it is assumed that the air pressure in the soil is in equilibrium with the atmosphere and at zero gage pressure. Note that the van Genuchten (1980) equations are used to

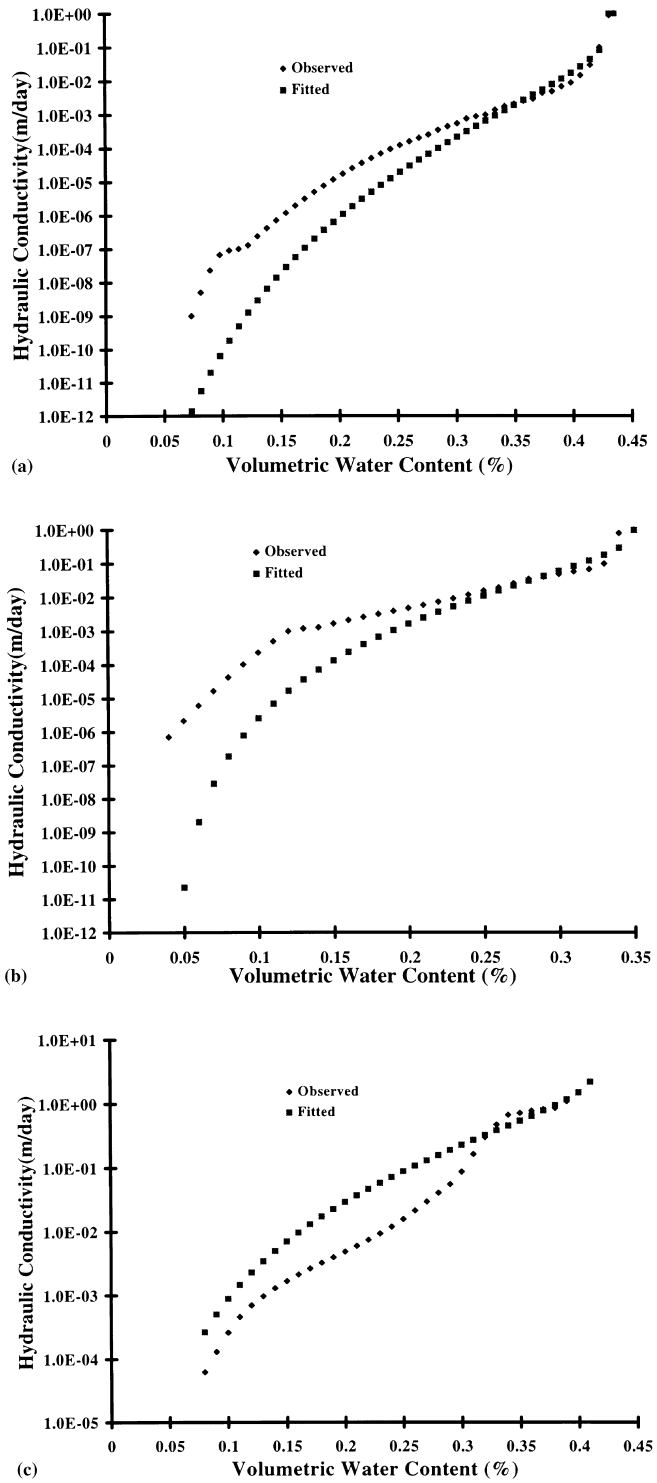

Fig. 4. The unsaturated hydraulic conductivity curve for (a) the humic layer.(b) the hydrophobic layer (c) the hydrophilic layer.

describe the water retention and hydraulic conductivity properties of the porous medium.

Eqs. 2(c)–(e) indicate that the hydraulic conductivity at a point in the air-dry soil will be zero until infiltrating water wets the porous medium up to the residual water content, θ_r. At air-dry water content, the water exists as disconnected islands in the porous medium. Liu et al. (1994) show that the wetting of the porous media starting from initially dry conditions occurs by erratic advances of the water–air interface. Since established models of unsaturated hydraulic conductivity do not apply to the case of discontinuous fluid volumes, it is assumed that hydraulic conductivity is zero for water contents less than the residual.

Scanning functions between the main drainage function and the boundary wetting scanning function are defined using the independent domain model of Mualem (1974).

The numerical solution of the Richards Eq. (1) uses the conventional Galerkin finite element method, presented by Nieber (1996). Eq. 1 includes strong non-linearity, namely the dependence of the unsaturated hydraulic conductivity and capillary pressure on water content. The modified Picard method was used to solve the discretized non-linear equations and the diagonal preconditioned conjugate gradient (PCG) method to solve the resulting quasilinearized matrix equations. Details of the numerical solution techniques can be found in Nieber (1996). The solution employs rectangular elements with weighting of the internodal hydraulic conductivities. Water retention and hydraulic conductivity relations were used as described by Eqs. 2(a)–(e).

The initial condition for soil water pressure in the finite element domain was determined by interpolating the measured values of water saturation and computing the soil water pressure head from the interpolated saturation. During the simulation time, the rate of rainfall was always smaller than the saturated hydraulic conductivity, we thus assumed that there was no runoff on the field site. The measured rainfall and evaporation data were imposed as boundary conditions at the top of the domain. No flow boundary conditions were applied along the vertical sides of the domain. An unit hydraulic gradient condition was applied at the lower boundary because the groundwater level was always lower than the bottom of the soil profile during the simulation period.

The finite element grid for the 2.2 m wide by 0.7 m deep solution domain was constructed using linear rectangular elements with vertical dimensions of 0.01 m and horizontal dimensions of 0.011 m. This construction led to a total of 14,000 grid points for the solution.

2.3. Model evaluation

To determine how well the numerical simulations of flow mimic the observed field data, visual comparisons of observed and simulated wetting patterns were performed. We also quantified differences between the simulated and observed results using statistical analyses of differences at discrete sampling points. For the statistical analyses, three measures of goodness of fit (e.g., Cooley, 1979, and Loague and Green, 1991) were used to quantify the accuracy of the simulation. The mathematical expression of these measures are given by Loague and Green (1991).

Mean difference (*MD*) between simulated and observed values

$$MD = \frac{1}{N}\sum_{i=1}^{N}(P_i - O_i) \tag{3}$$

Standard deviation for the mean difference between simulated and observed values (*S*)

$$S = \sqrt{\frac{\sum_{i=1}^{N}(P_i - O_i)}{N-1}} \tag{4}$$

Coefficient of determination (*CD*)

$$CD = \frac{\sum_{i=1}^{N}(O_i - \bar{O})^2}{\sum_{i=1}^{N}(P_i - \bar{O})^2} \tag{5}$$

Fig. 5. The simulated (sim.) and observed (Obs.) saturation patterns (a) for eight measurement times. (b) at the 98 TDR probes for eight measurement times.

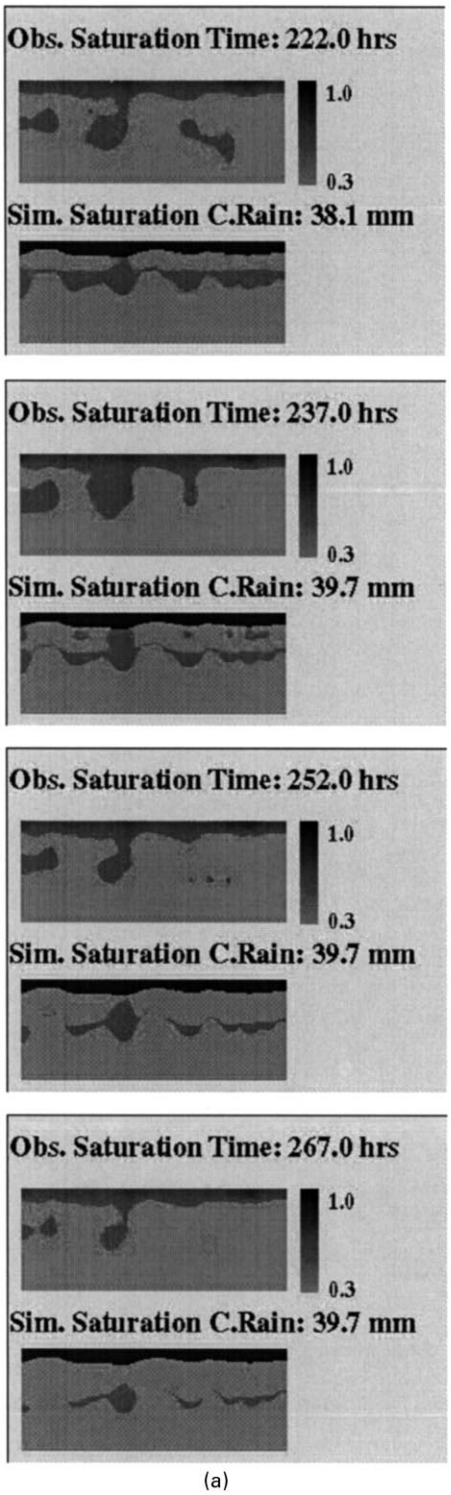
Obs. Saturation Time: 222.0 hrs
1.0
0.3
Sim. Saturation C.Rain: 38.1 mm
Obs. Saturation Time: 237.0 hrs
1.0
0.3
Sim. Saturation C.Rain: 39.7 mm
Obs. Saturation Time: 252.0 hrs
1.0
0.3
Sim. Saturation C.Rain: 39.7 mm
Obs. Saturation Time: 267.0 hrs
1.0
0.3
Sim. Saturation C.Rain: 39.7 mm

(a)

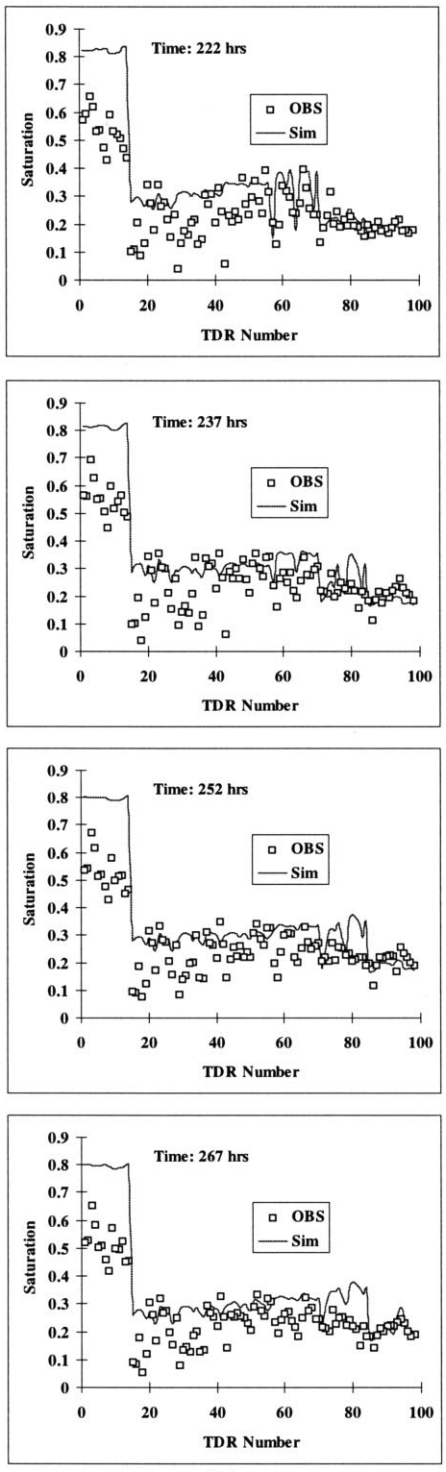
Time: 222 hrs
Time: 237 hrs
Time: 252 hrs
Time: 267 hrs
OBS
Sim
Saturation
TDR Number
0
0.1
0.2
0.3
0.4
0.5
0.6
0.7
0.8
0.9
0
20
40
60
80
100

(b)

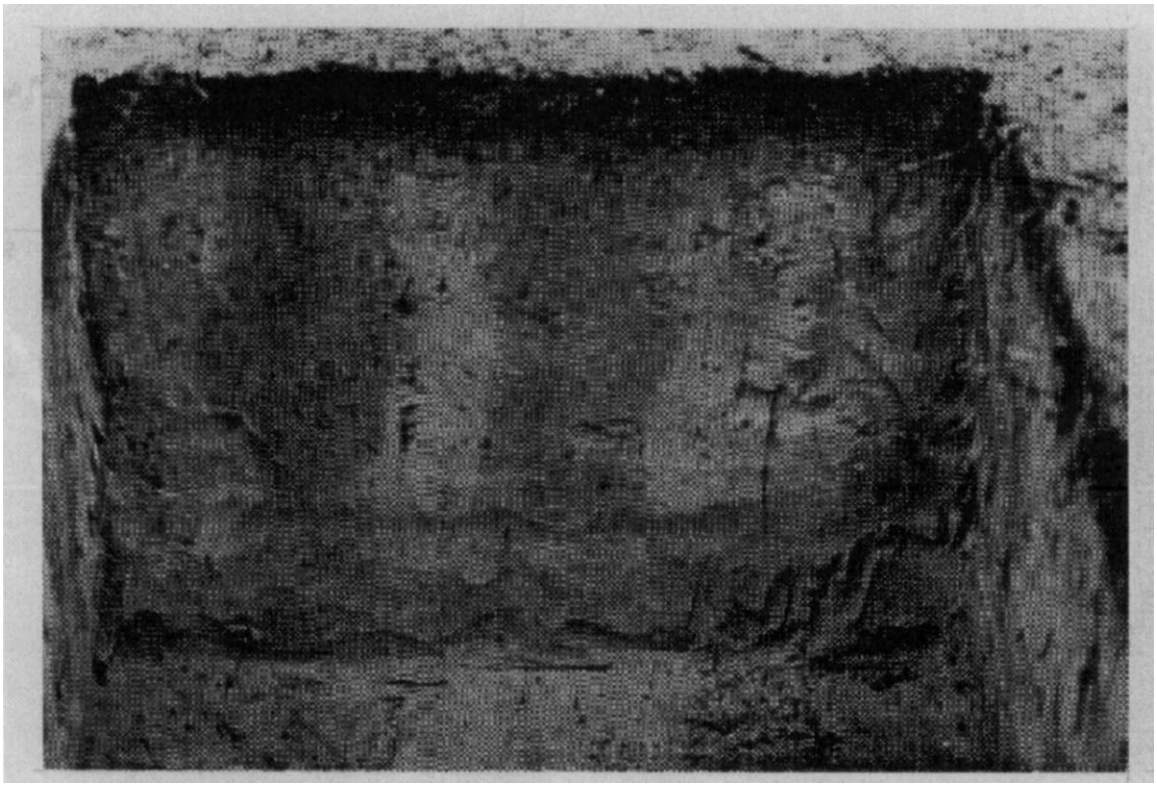

Fig. 6. Wet topsoil with vertical fingered flow paths below it (adapted from Ritsema and Dekker, 1993).

where O_i and P_i are the observed and simulated values, O is the mean of the observed values, and N is the number of samples. If all simulated values were equal to observed values *MD*, S, and *CD* would be 0.0, 0.0, and 1.0, respectively.

3. Results and discussion

3.1. Fingered flow patterns observed from the field

At a given time, water saturation patterns were calculated by the following procedure from field data. First, the soil water content at the 98 TDR probes were converted to saturation data. These saturation data were interpolated with kriging at the 14,000 grid points using SURFER 5.0 software. The interpolated saturations at the node points were used to compose raster images. Illustrations of the observed spatial pattern of water saturation in the trench are presented in Fig. 5(a). The reference time, time = 0.0 day, is 1:00 am on December 1, 1994, and represents the initial conditions used as input to the finite element simulation. Eight measurement times are shown. The incident rainfall cumulated up to the time corresponding to a given plot is shown on each inset figure. It is observed that following appreciable rainfall, fingered flow occurs. It can also be seen that after repeated rainfall events, fingers redevelop at the same location. This persistence of fingered flow pathways has been reported by Glass et al. (1989b), Van Dam et al. (1990), Ritsema and Dekker (1996), Ritsema et al. (1997), Ritsema et al. (1998) and Nieber (1996).

3.2. Simulated fingered flow patterns

The match between the simulated and observed fingered flow patterns may be examined qualitatively using visual comparison of contour maps of simulated

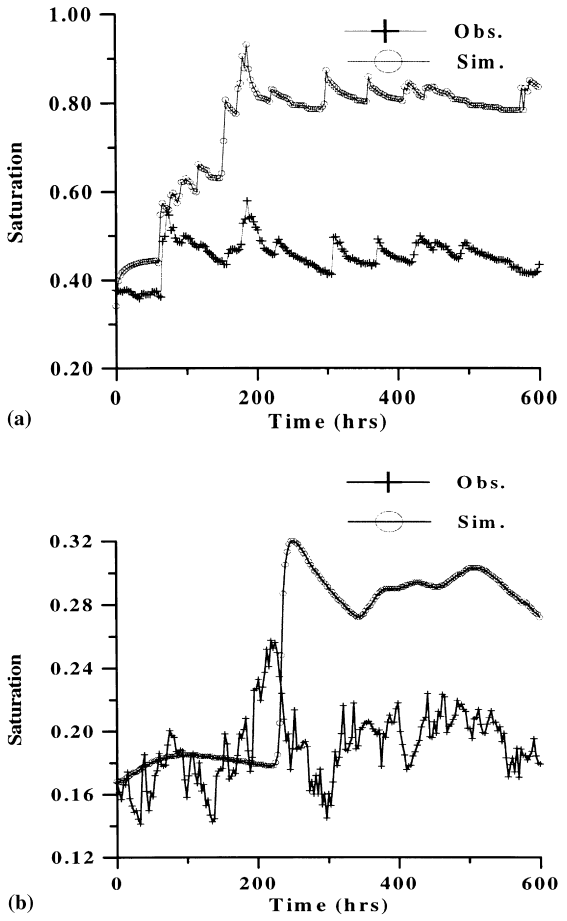

Fig. 7. Soil water saturation versus time at horizontal center with depth of (a)4 cm (humic layer).(b) 20 cm (hydrophobic layer).

and observed water saturation. Fig. 5(a) shows the comparison of fingered flow patterns for eight computational times selected from a period when a large rainfall event occurred (Fig. 2). The choice of this time period is based on the expectation that the variation in soil water content will be greatest during a period of significant rainfall. In addition to comparing the fingered flow patterns, we compared the simulated and observed water saturations at the 98 TDR sensors for each time step. Fig. 5(b) shows the simulated and observed saturations at 98 TDR sensors for eight simulation times. The 98 TDR sensors numbered sequentially along each row from left to right and from top to bottom. The first fourteen TDR sensors belonged to the humic layer, the next forty-two were in the hydrophobic layer and the rest in the hydrophilic layer. From the first two frames of Fig. 5(a) and Fig. 5(b), there is close agreement between the observed and simulated fingered flow patterns. However, the observed flow field shows faster finger propagation. The reason for this may be due to the lower hydraulic conductivity used in the simulation for the humic and hydrophobic layers (Fig. 4(a), Fig. 4(b)). Generally, the simulated saturation is higher than the observed saturation in the humic layer, but there is close agreement for the rest of the of the domain (the hydrophobic and hydrophilic layers). While there were differences between the simulated and observed saturation distributions, the similarity between the patterns is encouraging. In total, comparisons were made at 201 times and the similarities seen in Fig. 5(a) were also found in the remaining 193 times not shown.

The observed finger flow patterns merged in the hydrophobic layer at certain times (Fig. 5(a)) which does not happen in the field (Fig. 6). This may be due to insufficient data used in the interpolation. Unstable flows lead to quite discontinuous saturation distributions, and therefore attempting to describe the moisture distribution by interpolation from 98 TDR sensors is not completely adequate.

Fig. 7(a) and Fig. 7(b) show the soil water saturation versus simulation times at the center of the trench at depths of 4 and 20 cm. Fig. 7(a) shows clearly that simulated saturation was close to the observed, at the beginning of the simulation but gets bigger as the simulation proceeds in the humic layer. One possible reason for the over-prediction of simulated saturation in the humic layer may be due to the absence of a procedure in the model to account for the uptake of water in the root zone. Another possible reason is that measurements with TDR is less sensitive near saturation. However, in general, the simulated saturation values capture closely the fluctuating trend observed. In Fig. 7(b), there is a jump of simulated saturation at around a time of 210 hrs when a large rainfall event occurred, and from that time on the simulated saturations were higher than observed. Also, there is a delay in the appearance of the jump, and the slowed drainage (presumably resulting from the smaller unsaturated hydraulic conductivity used, Fig. 4(b)) may account for the increased simulated saturation. The observed saturations are more sensitive to the

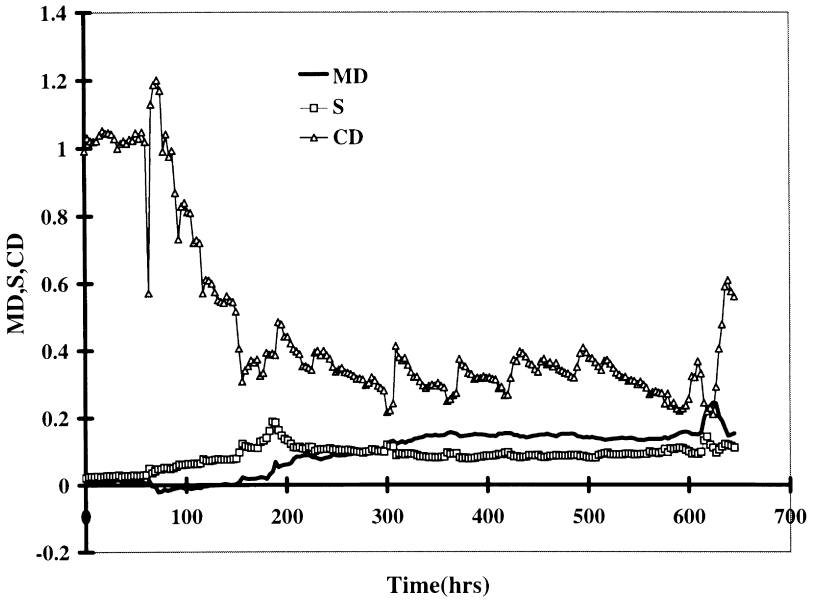

Fig. 8. Mean difference between simulated and observed saturation, standard deviation and the coefficient of determination versus simulation times.

change of rainfall or evaporation than the simulated saturations. Again, this may be due to the absence of routines in the code to handle evapotranspiration.

To quantify the accuracy of the simulation, the difference between simulated and observed values were used to evaluate model performance by characterizing, for example, systematic under- or over-prediction. Fig. 8 shows these measures, *MD*, S and *CD*, computed using Eqs. (3–5) applied to the observed and simulated saturation at all 98 TDR locations for 201 times. It can be seen that the variations of *MD* and S are small during the simulation period. There are some small sudden increases in the values of these parameters at times corresponding to large rainfall events. In general, the model over-predicted saturation as indicated by the predominance of positive values of *MD* during the simulation.

The *CD* is a measure of the proportion of the total variance of observed data explained by the simulated data. The value of *CD* oscillated during simulation times, illustrating the transient nature of model performance. The model performance was very good at early time (up to 60 hrs), as indicated by the value of *CD* being close to one and the values of *S* and MD being close to zero. After 60 hrs the performance of the model is fairly good, since *MD* and S remained relatively close to zero while the value of *CD* oscillated around 0.4. *MD*, S and *CD* fell within the respective ranges of - − 0.020 to 0.158, 0.002 to 0.188 and 0.216 to 1.201 respectively over the duration of the simulation. The average *MD*, S and *CD* for the comparison were 0.089, 0.081 and 0.464, respectively. These values indicated that the model predicted the observed moisture distributions reasonably well.

4. Summary and conclusions

The numerical solution for gravity-driven unstable flow described by Nieber (1996) is applied to the simulation of TDR measured moisture distributions in a 2.2 m wide by 0.7 m deep field trench located in the southwestern part of the Netherlands. The field soil contains a hydrophobic layer which causes the flow to become unstable during infiltration events. Visual comparisons of observed and simulated moisture distributions, and statistical measures of the comparison between point-wise observed and simulated moisture saturations are presented. The statistical

measures used included the mean difference between simulated and observed water saturation, the standard deviation of the mean difference, and the coefficient of determination between the simulated and observed water saturation.

The visual comparison of the observed and simulated water saturation distributions indicated that the simulation model was able to capture the main features of the unstable flow detectable in the observed data. The statistical measures indicate a fairly good agreement between the observed and simulated water saturations. The simulation model tended to over-predict the observed saturation, and this is thought to be related to either the lack of an evapotranspiration algorithm in the model, or to the under-prediction of the measured unsaturated hydraulic conductivity with the van Genuchten equations.

Acknowledgements

Published as Paper No. 981120022 of the scientific journal series of the Minnesota Agricultural Experiment Station on research conducted under Minnesota Agricultural Experiment Station Project No. 12-047. Experimental work was supported by the Environment Research Programme of the European Union (EV5V-CT94-0467), Research Programme 223, 'Physical Soil Quality', of the Dutch Ministry of Agriculture, Nature Management and Fisheries, and the Netherlands Integrated Soil Research Programme (C3–13). The modeling part was supported by the Army High Performance Computing Research Center under the auspices of the Department of the Army, Army Research Laboratory cooperative agreement number DAAH04-95-2-0003/contract number DAAH04-95-C-0008, the content of which does not necessarily reflect the position or the policy of the government, and no official endorsement should be inferred. Collaboration on the research was supported by the NATO Collaborative Research Grant No. 960704.

References

Beven, K., 1991. Modeling preferential flow: An uncertain future. In: Gish, T.J., Shirmohammadi, A. (Eds.). Preferential flow. Proceeding of the national symposium, Chicago, Illinois, U.S.A. 16-17 Dec. 1991., American Soc.Of Agricultural Engineers, St. Joseph, Michigan, USA, pp. 1–11.

Cooley, R.L., 1979. A method of estimating parameters and assessing reliability for models of steady state groundwater flow, 2: application of statistical analysis. Water Resour. Res. 15, 603–617.

Dalen, V., 1976. Immiscible flow by finite elements. In: First Int. Intern. Conference on Finite Elements in Water Resources, pp. 3.69-3.90.

Dekker, L.W., Ritsema, C.J., 1994. How water moves in a water repellent sandy soil: 2. Dynamics of fingered flow. Water Resour. Res. 30, 2507–2517.

Ghodrati, M., Jury, W.A., 1990. A field study using dyes to characterize preferential flow of water. Soil Sci. Soc. Am. J. 54, 1558–1563.

Glass, R.J., Steenhuis, T.S., Parlange, J.-Y., 1988. Wetting front instability as a rapid and far-reaching hydrologic processes in the vadose zone . J. Contam. Hydrol. 3, 207–226.

Glass, R.J., Parlange, J.-Y., Steenhuis, T.S., 1989a. Wetting front instability. 2. Experimental determination of relationships between system parameters and two-dimensional unstable flow field behavior in initially dry porous media. Water Resour. Res. 25, 1195–1207.

Glass, R.J., Steenhuis, T.S., Parlange, J.-Y., 1989b. Mechanium for finger persistence in homogenerous. unsaturated porous media: Theory and verification. Soil Science 148, 60–70.

Green, W.H., Green, W.H., Ampt, G.A., 1911. Studies in soil physics. I. The flow of air and water through soils. J. Agr. Sci. 4, 1–24.

Hendrickx, J.M.H., Dekker, L.W., 1991. Experimental evidence of unstable wetting fronts in homogeneous non-layered soils. In: Gish, T.J., Shirmohammadi, A. (Eds.). Proceedings of the national Symposium on Preferential Flow, Dec. 16-17, Chicago, Illinois, American Soc. Of Agricultural Enginers, St. Joseph, Michigan, USA, pp. 22–31.

Hendrickx, J.M.H., Dekker, L.W., Boersma, O.H., 1993. Unstable wetting fronts in water repellent field soils. J. Envir. Qual. 22, 109–118.

Jamison, V.C., 1945. The penetration of irrigation and rain water into sandy soils of central Florida. Soil Sci. Soc. Amer. Proc. 10, 25–29.

Klute, A., 1986. Methods of soil analysis. 1. Physical and mineralogical methods. Agronomy 9, ASA, SSSA, Madison,WI part 1.

Liu, Y., Steenhuis, T.S., Parlange, J.-Y., 1994. Formation and persistence of fingered flow in coarse grained soils under different moisture contents. J. Hydrol. 159, 187–195.

Loague, K.M., Green, R.E., 1991. Statistical and graphical methods for evaluating solute transport models: overview and application. J. Contam. Hydrology vol. 7, 51–73.

Mualem, Y., 1974. A conceptual model of hysteresis. Water Resour. Res 10, 514–520.

Nieber, J.L., 1996. Modeling finger development and persistence in initial dry porous media. Geoderma 70, 209–229.

Pendexter, W.S., Furbish, D.J., 1991. Development of a heterogeneous moisture distribution and its influence on the evolution of preferred pathways of flow in an unsaturated sandy soil. In:

Gish, T.J., Shirmohammadi, A. (Eds.). Preferential flow. Proceeding of the national symposium, Chicago, Illinois, U.S.A. 16-17 Dec. 1991, American Soc. Of Agricultural Engineers, St. Joseph, Michigan, USA, pp. 104–112.

Philip, J.R., 1969. Theory of infiltration. In advances in hydroscience, Academic Press, New York, 215–296.

Philip, J.R., 1975. Stability analysis of infiltration. Soil Sci. Soc. Am. Proc. 39, 1042–1049.

Ritsema, C.J., Dekker, L.W., 1993. Preferential flow mechanism in a water repellent sandy soil. Water Resour. Res. 29, 2183–2193.

Ritsema, C.J., Dekker, L.W., 1996. Water repellency and its role in forming preferred flow paths in soil. Aust. J. Res. 34, 475–487.

Ritsema, C.J., Steenhuis, T.S., Parlange, J.-Y., Dekker, L.W., 1996. Predicted and observed finger diameters in field soils. Geodema 70, 185–196.

Ritsema, C.J., Dekker, L.W., van der Elsen, E.G.M., Oostindie, K., Steenhuis, T.S., Nieber, J.L., 1997. Recurring fingered flow pathways in a water repellent sandy field soil . J. of Hydrology and Earth System Sciences 4, 777–786.

Ritsema, C.J., Dekker, L.W., Nieber, J.L., Steenhuis, T.S., 1998. Modeling and field evidence of finger formation and finger recurrence in a water repellent sandy soil. Water Resour. Res. 34, 555–567.

Starr, J.L, DeRoo, H.C., Frink, C.R., Parlange, J.-Y., 1978. Leaching characteristics of a layered field soil. Soil Sci. Soc. Am. J. 42, 386–391.

Stolte, J., Veerman, G.J., Wopereis, M.C.S., 1992. Manual soil physical measurements, version 2.0. DLO Winand Staring Center, Wageningen, Technical Document 2, 49pp.

Tamari, S., Bruckler, L., Halbertsma, J., Chadoeuf, J., 1993. A simple method for determining soil hydraulic properties in the laboratory. Soil Sci. Soc. Am. J. 57, 642–651.

van Dam, J.C., Hendrickx, J.M.H., van Ommen, H.C., Bannink, M.H., van Genuchten, M.Th., Dekker, L.W., 1990. Water and solute movement in a coarse-textured water-repellent field soil. J. Hydrol. 120, 359–379.

van Genuchten, M.Th., 1980. A closed form equation for predicting the hydraulic conductivity of unsaturated soils. Soil Sci. Soc. Am. J. 44, 892–898.

van Genuchten, M. Th., Leij, F.J., Yates, S.R., 1991. The RETC code for quantifying the hydraulic functions of unsaturated soils, EPA/600/2-91/065. 93pp. R.S. Kerr Environ. Res. Lab. U.S. Environmental projection Agency, Ada, OK.

van Ommen, H.C., Dekker, L.W., Dijksma, R., Hulshof, J., van der Molen, W.H., 1988. A new technique for evaluating the presence of preferential flow paths in non-structured soils. Soil Sci. Soc. Am. J. 52, 239–245.